References

1. C. ZENER, *J. Appl. Phys.* **20** (1949) 950.
2. H. B. AARON and H. I. AARONSON, *Acta Met.* **16** (1968) 789.
3. A. D. BRAILSFORD and H. B. AARON, *J. Appl. Phys.* **40** (1969) 1702.
4. R. G. FAULKNER and J. CAISLEY, *Metal Sci.* **11** (1977) 200.
5. S. J. SANDERSON, *ibid.* **11** (1977) 23.
6. J. P. ADAMSON, D. Phil. Thesis, University of Oxford (1972).
7. C. da CASA, V. B. NILESHWAR and D. A. MELFORD, *J. Iron and Steel Inst.* **207**. (1969) 1325.
8. M. DEIGHTON, *ibid.* **208** (1970) 1012.
9. B. AARONSON, Proceedings of the Conference on "Steel Strengthening Mechanisms" (Climax Molybdenum Co., Greenwich, Conn., 1969) p. 77.
10. A. F. SMITH and G. B. GIBBS, *Metal Sci. J.* **3** (1969) 93.
11. B. SPARKE, D. W. JAMES and G. M. LEAK, *J. Iron and Steel Inst.* **203** (1965) 152.
12. M. DEIGHTON, *ibid.* **205** (1967) 535.
13. S. H. MOLL and R. E. OGILVIE, *Trans. Met. Soc. AIME* **215** (1959) 613.
14. F. R. BECKETT and T. GLADMAN, BSC Research Report SSD 818 (1972).

Received 18 October 1978
and accepted 21 February 1979.

R. G. FAULKNER
Department of Materials Engineering and Design, University of Technology, Loughborough, Leicestershire, UK

Hot hardness of SiC single crystal

Silicon carbide (SiC) is one of the hardest and most refractory materials and is of considerable interest as a high-temperature structural material [1]. Hardness is an important factor in the choice of ceramics for abrasives, tool bits, bearings and wear resistant coatings, and it generally correlates with both micro- and macro-plastic deformation and with the ease of machining [2]. In the case of SiC, the room temperature hardness has been examined in some detail [3–6], whereas the knowledge of high-temperature hardness (hot hardness) is quite limited [7, 8]. Up to now no attempt has been made to analyse the hot hardness of SiC single crystals. In this work, the Vickers microhardness (VMH) tests were made on the basal plane and two kinds of prismatic planes ($\{1\,0\,\bar{1}\,0\}$ and $\{1\,1\,\bar{2}\,0\}$) of the single crystal of 6H-polytype SiC, from room temperature up to 1500° C. The creep behaviour at high temperatures was also investigated by hardness measurements at high temperatures.

6H-SiC single crystals were grown from melts of silicon, carbon and sodium chloride [9]. The planes for hardness tests were polished by various grades of diamond paste (3 to 0.25 μm). Hardness measurements were made using a high-temperature micro-hardness tester (Nikon, Model QM) in a vacuum of 1×10^{-5} to 5×10^{-4} Torr [10]. In almost all measurements, 100 g loads were applied for 10 sec at a lowering rate of 0.3 mm sec^{-1}. Loads of 25 to 500 g and loading times of 0.1 sec to 1 h were used for observations of the deformation behaviour around indentations and for creep tests, respectively. The VMH values reported in this work represent the average of at least 10 indentation measurements. The failure of diamond indenter's tip by chemical reaction, mechanical fracture and graphitization [11] was not observed.

Fig. 1 shows the temperature dependence of VMH at a 100 g load on (0 0 0 1), $\{1\,0\,\bar{1}\,0\}$ and $\{1\,1\,\bar{2}\,0\}$ planes a 6H-SiC single crystal. Measurements were performed when one of the indenter diagonals was aligned $\langle 1\,0\,\bar{1}\,0\rangle$ on the basal plane and [0 0 0 1] on the prismatic planes. The random errors in these measurements were considerably reduced with increasing temperature

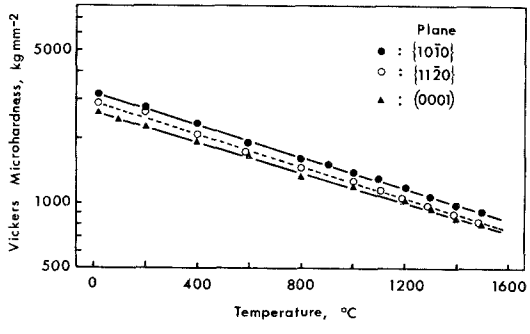

Figure 1 Temperature dependence of Vickers microhardness for the (0 0 0 1), $\{1\,0\,\bar{1}\,0\}$ and $\{1\,1\,\bar{2}\,0\}$ planes of 6H-SiC single crystal (100 g load).

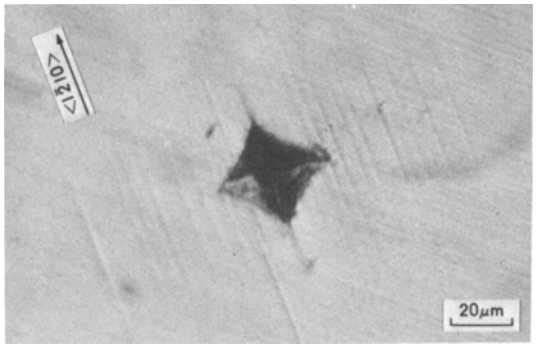

Figure 2 Slip produced by a Vickers microhardness indentation under the condition of 300 g load and 1500° C for the $\{1\,0\,\bar{1}\,0\}$ plane of 6H-SiC single crystal.

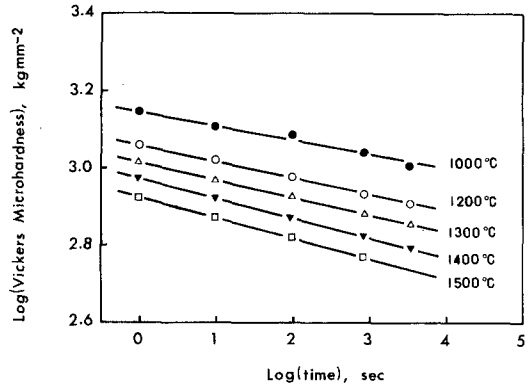

Figure 3 Variation in Vickers microhardness with the loading time for the $\{1\,0\,\bar{1}\,0\}$ plane of 6H-SiC single crystal (200 g load).

and lie within the extent of the data points at high temperatures above 1000° C, while they were within ± 120 kg mm^{-2} near room temperature.

As is evident from Fig. 1, the logarithmic VMH decreased linearly with increasing temperature in the same manner as various other materials [11, 12]. 6H-SiC, however, retains a high hot-hardness of 800 ~ 910 kg mm^{-2} at 1500° C and shows considerably lower softening rates compared with those of representative hard materials such as TiC, W_2C, TiB_2, ZrB_2, HfB_2 and Al_2O_3 [10–13]. Moreover, the value of VMH varies depending on the crystallographic plane as shown in Fig. 1. The VMH was highest on the prismatic plane $\{1\,0\,\bar{1}\,0\}$ and lowest on the basal plane throughout all the testing temperatures.

Star-like cracks observed at the corners of indentations diminished with increasing temperature above 800° C. At higher loads of more than 300 g, however, the cracks occurred even at 1500° C. As shown in Fig. 2, the slip lines were observed around indentations above 800° C, which increased substantially with increasing temperature. This may imply that the plasticity of 6H-SiC increases rapidly at temperatures above 800° C.

The variation in VMH with the loading time (creep of VMH) was measured for the basal and prismatic planes at temperatures between 1000 and 1500° C. Typical results are shown in Fig. 3. A linear relationship was obtained between log(VMH) and log(time). It is thought very likely that the slope gradually increases with increasing temperature up to 1300° C and is independent of temperature above 1400° C.

The hardness creep in the temperature range above 0.5 T_m (where T_m is the absolute melting temperature) has usually been analysed in terms of transient creep, and the following equation [10, 14] is given for the relation between hardness (H) and loading time (t):

$$K_1/t = H^m \exp(-Q/RT) \qquad (1)$$

where K_1 and m are constants, R is the gas constant and Q is the activation energy for creep.

The Q value for the hardness creep calculated from the data at 1400 and 1500° C (above 0.6 T_m) in Fig. 3, using Equation 1, was 125 ± 10 kcal mol^{-1}, independent of the crystallographic plane. The value is close to the activation energy of 140 kcal mol^{-1} for the lattice diffusion of carbon in SiC single crystals [15]. Thus, it may be concluded that at temperatures above 0.6 T_m the creep process of 6H-SiC single crystal is dominated by a self-diffusion mechanism as is the case for other various materials [7, 10, 11, 14].

For the sintered polycrystalline SiC (3% porosity), Atkins and Tabor [7] measured the hardness creep using a mutual-indentation technique, and obtained the Q value of 45 kcal mol^{-1} at 0.5 T_m, which is smaller than that for the 6H-SiC single crystal obtained in this work. Their value for the sintered SiC, however, seems to be comparable with the activation energies, 73 and 55 kcal mol^{-1} for the grain boundary diffusion of carbon [15] and for the bending creep process controlling by the build-up of stresses produced by grain boundary sliding [16], respectively.

Acknowledgement

This research was supported in part by a scientific research grant from the Ministry of Education, under Contract Nos 285168 and 265212.

References

1. D. J. GODFREY, *Metals and Materials* **2** (1968) 305.
2. R. N. KATZ and E. M. LENOE, "Treatise on Materials Science and Technology, Vol. 9, Ceramic Fabrication Processes", (Academic Press, New York, 1976) p. 241.
3. P. T. B. SHAFFER, *J. Amer. Ceram. Soc.* **47** (1964) 466.
4. O. O. ADEWOYE and T. F. PAGE, *J. Mater. Sci.* **11** (1976) 981.
5. E. H. VOICE and V. C. SCOTT, "Special Ceramics 5", edited by P. Popper (British Ceramic Research Association, Stoke-on-Trent, 1972) p. 1.
6. D. J. GODFREY and K. C. PITMAN, "Ceramic for High Performance Applications", edited by J. J. Burke, A. E. Gorum and R. N. Katz (Brook Hill, Massachusetts, 1974) p. 425.
7. A. G. ATKINS and D. TABOR, *Proc. Roy. Soc.* **A292** (1966) 441.
8. L. M. FITZGERALD, *J. Less-Common Metals* **5** (1963) 356.
9. K. NIIHARA, *ibid.* **65** (1979) 155.
10. Y. KUMASHIRO, A. ITOH, T. KINOSHITA and M. SOBAJIMA, *J. Mater. Sci.* **12** (1977) 595.
11. D. L. KOHLSTEDT, *ibid.* **8** (1973) 777.
12. L. BSENKO and T. LUNDSTROM, *J. Less-Common Metals* **34** (1974) 273.
13. R. D. KOESTER and D. P. MOAK, *J. Amer. Ceram. Soc.* **50** (1967) 290.
14. A. G. ATKINS, A. SILVERIO and D. TABOR, *J. Inst. Metals* **94** (1966) 369.
15. P. L. FARNSWORTH and R. L. COBLE, *J. Amer. Ceram. Soc.* **49** (1966) 264.
16. P. MARSHALL and R. B. JONES, *Powd. Met.* **12** (1968) 193.

Received 3 November
and accepted 14 November 1978.

T. HIRAI
K. NIIHARA
The Research Institute for Iron, Steel and Other Metals, Tohoku University, Sendai 980, Japan

Ternary tantalate compositions

The purpose of this communication is to present refined powder X-ray diffraction data and some properties of tantalates selected for a previous study [1] of possible low thermal expansion oxides. Four ternary* $A^{3+}B^{4+}C^{5+}O_6$ compounds were prepared, $AlTiTaO_6$, $AlHfTaO_6$, $YTiTaO_6$, and $YHfTaO_6$. Of these, $AlTiTaO_6$ and $YTiTaO_6$ had been previously studied [2, 3], but no powder X-ray diffraction data were available for them.

These oxides were prepared by co-hydrolysis to the mixed metal hydroxides from solutions of the respective metal alkoxides, using starting materials nominally of $\geqslant 99\%$ purity. Co-precipitated products were vacuum-dried and calcined for 40 h at 800 to 1000° C in air. Calcined powders were isostatically pressed into rods and sintered at a temperature ~20 to 30% below the melting point in argon.

Specimens were analysed chemically (X-ray fluorescence), their densities were measured by mercury intrusion porosimetry, and their melting points were determined by differential thermal analyses. Electrical resistivities were obtained with a digital multimeter or megohmmeter, and thermal expansion was determined with a fused silica pushrod dilatometer. Preparation of samples and property determinations have been discussed in more detail elsewhere [1].

The powder X-ray diffraction (XRD) patterns were obtained from a 114.6 mm Debye–Scherrer camera (with Cu$K\alpha$ radiation) and were corrected for film shrinkage. A densitometer† scan was made of each film, and integrated intensities recorded with a digitiser‡. Lattice constants were refined by a least squares fit to the Nelson–Riley extrapolation function [4]. Theoretical densities were calculated from refined lattice parameters. The structure types were determined by comparison of observed diffraction data with reported data for analogous structures. The structure types and

*With respect to cations or systems (i.e. $A_2O_3 \cdot 2BO_2 \cdot C_2O_5$).
†GAF Model 652.
‡Hewlett-Packard 9821A Calculator with Model 20 Digitizer Pac.

0022–2461/79/092255–06 $02.60/0